ELSEVIER

Contents lists available at ScienceDirect

# Archives of Biochemistry and Biophysics

journal homepage: www.elsevier.com/locate/yabbi





# Probing the site of glutathione reduction by thioredoxin/glutathione reductase from *Schistosoma mansoni* under anaerobic conditions

Tyler B. Alt, Madison M. Smith, Graham R. Moran

Department of Chemistry and Biochemistry, 1068 W Sheridan Rd, Loyola University Chicago, Chicago, IL, 60660, USA

#### ARTICLE INFO

Handling editor: H Forman

Keywords:
Flavin adenine dinucleotide (FAD)
Nicotinamide adenine dinucleotide phosphate
(NADP/NADPH)
Disulfide exchange
Redox
Glutathione
Thioredoxin
Transient-state kinetics

#### ABSTRACT

Thioredoxin/glutathione reductase from Schistosoma mansoni (SmTGR) is a multifunctional enzyme that catalyzes the reduction of glutathione (GSSG) and thioredoxin, as well as the deglutathionylation of peptide and nonpeptide substrates. SmTGR structurally resembles known glutathione reductases (GR) and thioredoxin reductases (TrxR) but with an appended N-terminal domain that has a typical glutaredoxin (Grx) fold. Despite structural homology with known GRs, the site of GSSG reduction has frequently been reported as the Grx domain, based primarily on aerobic, steady-state kinetic measurements and x-ray crystallography. Here, we present an anaerobic characterization of a series of variant SmTGRs to establish the site of GSSG reduction as the cysteine pair most proximal to the FAD, Cys154/Cys159, equivalent to the site of GSSG reduction in GRs. Anaerobic steadystate analysis of U597C, U597S, U597C + C31S, and I592STOP SmTGR demonstrate that the Grx domain is not involved in the catalytic reduction of GSSG, as redox silencing of the C-terminus results in no modulation of the observed turnover number ( $\sim 0.025 \, \mathrm{s}^{-1}$ ) and redox silencing of the Grx domain results in an increased observed turnover number ( $\sim 0.08 \text{ s}^{-1}$ ). Transient-state single turnover analysis of these variants corroborates this, as the slowest rate observed titrates hyperbolically with GSSG concentration and approaches a limit that coincides with the respective steady-state turnover number for each variant. Numerical integration fitting of the transient state data can only account for the observed trends when competitive binding of the C-terminus is included, indicating that the partitioning of electrons to either substrate occurs at the Cys154/Cys159 disulfide rather than the previously proposed Cys596/Sec597 sulfide/selenide. Paradoxically, truncating the C-terminus at Ile592 results in a loss of GR activity, indicating a crucial non-redox role for the C-terminus.

### 1. Introduction

Flavoprotein disulfide reductases (FDRs) transmit electrons from NAD(P)H to disulfide substrates. In doing so FDRs transduce the form of reducing power from the NAD(P)H dihydronicotinamide to a dithiol. The oxidant substrate for an FDR enzyme can be unique to the reaction catalyzed or a more general redox active disulfide that has diverse cellular functions. Enzymes that catalyze the reduction of pervasive disulfides such as glutathione (GSSG), cystine, or thioredoxin (Trx) function to maintain cellular redox status by providing a channel to move electrons from primary catabolism to the thiol pool and back. While the reduction potential of NAD(P)H is  $\sim$ 100 mV more negative that of the recipient disulfide, dictating that these reactions are biased toward production of the dithiol, the concentration of intracellular thiols is high relative to NAD(P) so FDR enzymes presumably help to buffer the net redox status of the cell [1,2].

Parasitic platyhelminths (flatworms) of the genus *Schistosoma* are uniquely dependent on maintenance of reduced states of GSSG and Trx. Lacking catalase, they are limited to ameliorating hydrogen peroxide generated from the host immune response by recycling peroxiredoxins [3]. To accomplish this, these organisms employ a dual functional FDR known as thioredoxin/glutathione reductase (TGR, SmTGR from *Schistosoma mansoni*). Suppression of this enzyme in *Schistosoma mansoni* by iRNA has been shown to efficiently kill the parasite, establishing TGR as a drug target for the treatment of schistosomiasis [4], a disease endemic to many tropical and subtropical areas.

The structure of TGR closely resembles that of glutathione reductase (GR) and thioredoxin reductase (TrxR) [5–9]. Similarity to GR includes the NAD(P)H oxidizing machinery that is common to Class 1 FDR enzymes [10]. This includes a NAD(P)H nicotinamide binding pocket adjacent to the *re*-face of the flavin isoalloxazine and a proximal disulfide (Cys154, Cys159 in SmTGR) stacked against the *si*-face (Fig. 1). This

E-mail address: gmoran3@luc.edu (G.R. Moran).

<sup>\*</sup> Corresponding author.

arrangement relays two electrons from NAD(P)H to the disulfide via the flavin. In GR the GSSG binding site is directly near this recipient disulfide and GSSG becomes reduced by facile disulfide exchange [11]. TrxR differs from GR as it incorporates a C-terminal disulfide that resides at the end of a disordered  $\sim\!20$  residue segment of peptide. The redox pair at the C-terminus of TrxR is frequently a selenide-sulfide [7]. This moiety is believed to stochastically interact with the disulfide/dithiol adjacent the flavin; transiently interacting in the site where GSSG binds in GR and the site of the disulfide/dithiol of Trx that is  $\sim\!20$  Å distant from the flavin when Trx is bound (Fig. 1) [12].

TGR has all the reactive structural components of TrxR with the addition an N-terminally appended domain that has the fold of a Grx (shown in green in Fig. 1). This domain has a single disulfide (Cys28, Cys31 in SmTGR) that, while far from settled, has been proposed to be the primary site of GSSG reduction [8,13]. The proposal has been that the reduced C-terminal disulfide (or selenide-sulfide) can serve a dual role, extending to reduce either Trx or the N-terminal disulfide that are estimated to be ~50 Å apart in their respective binding sites. The primary evidence for the site of GSSG reduction in TGR is a GSH molecule bound near the Cys28-Cys31 dithiol of the Grx domain of U597C SmTGR (PDB 2X99). Glutaredoxins harvest electrons from glutathione to reduce numerous cellular entities including peroxiredoxins [14]. The Grx fold of the N-terminal domain of TGR would appear to be a modular structural appendage that was reasonably proposed to add the capacity for GSSG interaction and reduction. Aspects of this arrangement seem ambiguous and/or counterintuitive however, as such an activity places an intervening GSSG reduction and reoxidation in place of direct peroxiredoxin reduction by the reduced Grx domain of TGR. Moreover, Grxs are typically reduced by GSH without complexation (presumably because the intervening mixed disulfide is sufficient tethering to promote the reaction), yet the 2X99 structure of U597C SmTGR has GSH bound near the Cys28-Cys31 dithiol suggesting that its function is distinct from a typical Grx [9]. Using cysteine variants of TGR, we show the rate of GSSG reduction is unchanged with redox silencing of the C-terminal selenide-sulfide (Cys596, Sec597) and is increased with redox silencing of the disulfide of the appended Grx domain (Cys28, Cys31). We propose that the site of GSSG reduction in TGR is instead equivalent to that of GR and that GSSG competes with the C-terminal disulfide for access to the dithiol most proximal to the flavin si-face such

that partitioning of electrons to GSSG or Trx occurs at the first disulfide pair of the TGR disulfide exchange relay (Cys154, Cys159) and not at the C-terminal sulfide-selenide (Cys596, Sec597) as has been proposed.

#### 2. Methods

Materials and Quantitation: Oxidized nicotinamide adenine dinucleotide phosphate (NADP $^+$ ), dipotassium hydrogen phosphate (KPi), isopropyl- $\beta$ -thiogalactopyranoside (IPTG), ethylenediaminetetraacetic acid (EDTA), the Miller formulation of lysogeny broth (LB) powder, and sodium dodecylsufate (SDS) were obtained from Fisher Scientific. Lysogeny Broth (LB) agar tablets were from Bio101 Inc. Competent BL21 (DE3) *Escherichia coli* cells were acquired from New England BioLabs. Reduced nicotinamide adenine dinucleotide phosphate (NADPH) was purchased from RPI Research Products. Flavin adenine dinucleotide (FAD) was from Acros. Talon superflow resin was obtained from Cytvia. Kanamycin was purchased from Alfa Aesar. Reduced nicotinamide adenine dinucleotide (NADH) was purchased from Amresco.

Where possible, concentrations were determined spectrophotometrically using the following extinction coefficients: NADPH;  $\epsilon_{340}=6220~\text{M}^{-1}\text{cm}^{-1}$ , NADP+;  $\epsilon_{260}=17,800~\text{M}^{-1}\text{cm}^{-1}$ , thioredoxin (SmTrx);  $\epsilon_{280}=9500~\text{M}^{-1}\text{cm}^{-1}$ , SmTGR U597C;  $\epsilon_{463~\text{nm}}=11,700~\text{M}^{-1}\text{cm}^{-1}$ , SmTGR U597C, C159S;  $\epsilon_{445~\text{nm}}=12,600~\text{M}^{-1}\text{cm}^{-1}$ , SmTGR U597S;  $\epsilon_{463~\text{nm}}=11,500~\text{M}^{-1}\text{cm}^{-1}$ , SmTGR U597C + C31S;  $\epsilon_{463~\text{nm}}=11,300~\text{M}^{-1}\text{cm}^{-1}$ , I592STOP SmTGR;  $\epsilon_{463~\text{nm}}=11,500~\text{M}^{-1}\text{cm}^{-1}$ . Extinction coefficients for variant forms of SmTGR were determined as previously described [15]. The concentration of oxidized glutathione was defined by weight. All reactant concentrations indicated in this text are post-mixing. All experiments were performed in 50 mM KPi, pH 7.4, at 20 °C.

Expression and purification of SmTGR variants and SmTrx: Expression and purification of SmTGR variants, and SmTrx were achieved using modest revisions of protocols previously described [15,16]. Genes for S. mansoni TGR U597C and Trx were synthesized and subcloned into the pET28a(+) expression plasmid by Genscript using NdeI and XhoI restriction sites to give the plasmids pSmTGR and pSmTrx respectively, placing both genes in phase with the sequence coding for an N-terminal 6His-tag linked by a thrombin cleavage site. Mutant SmTGR genes derived from pSmTGR were prepared and validated by

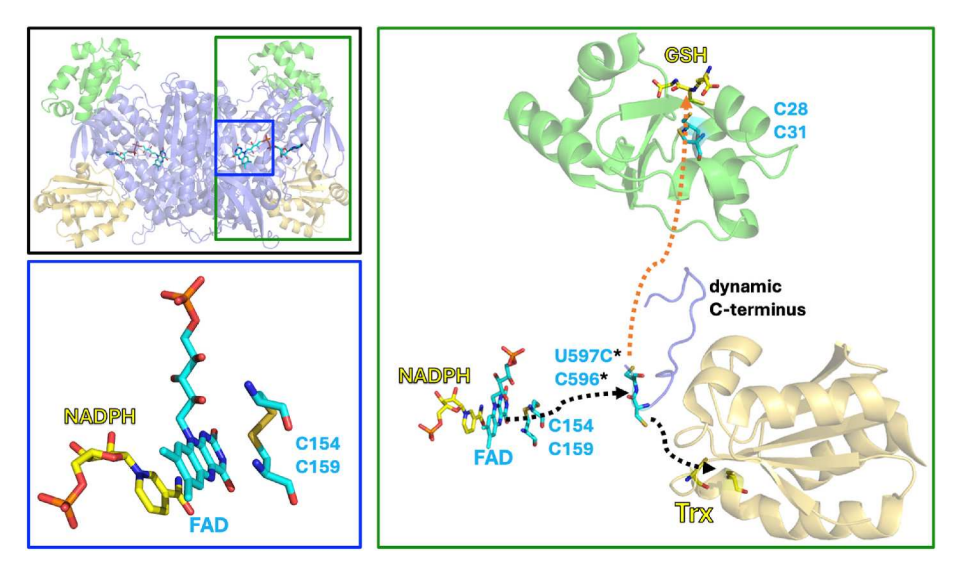


Fig. 1. The proposed disulfide exchange electron relay of SmTGR. The figure shown is not data. This figure depicts the proposed spatial arrangement of redox active moieties in SmTGR and substrate/product ligands. The composite figure is formed from SmTGR structure PDB 2X8C (blue residues with periwinkle secondary structure with the exception of the N-terminal glutaredoxin-fold domain that is rendered in green), with ligand NADPH and GSH shown in yellow from the SmTGR structure PDB 2X99. Thioredoxin is shown from the structure of Plasmodium falciparum thioredoxin reductase from PDB 4J56. The high degree of fold similarity facilitated the assumed placement of each component by alignment of all three structures. Residues superscripted with an asterix are derived from the opposing subunit of the dimer. The validity of the disulfide exchange reaction depicted as an orange dashed arrow is the subject of this study.

Genscript. Expression plasmids were separately transformed into competent BL21 (DE3) *E. coli* cells. Cell stocks were prepared by transferring a single colony to an LB growth culture with 25  $\mu g/mL$  kanamycin and incubated at 37 °C, with shaking at 220 rpm until the culture showed initial signs of turbidity. Cell stocks were prepared by aliquoting 400  $\mu L$  of 0.22  $\mu m$  filtered 50 % glycerol with 600  $\mu L$  of the culture and stored at -80 °C.

To express SmTGR variants and SmTrx, the respective cell stock was spread onto an LB agar plate with 25 µg/mL kanamycin selection and incubated for 16 h at 37°C. The cells were resuspended with sterile LB broth and used to inoculate 1 L of LB with 25 µg/mL kanamycin selection. Cells were grown with shaking at 220~rpm at  $37^{\circ}\text{C}$  to an optical density at 600 nm of 0.8. The temperature of incubation was lowered to 25°C for an hour before inducing expression by the addition of 100 μM ITPG. The culture was then incubated at 25°C with shaking for 20 h. Purification was carried out at 4°C. Cells were harvested by centrifugation at 3500 g for 35 min and resuspended in 50 mM KPi and 100 mM NaCl, 50 μM FAD, pH 7.4 (~20 mL/L of expression culture) and incubated for 10 min. A Branson 450 sonifier set to 40 W was used to lyse the cells by sonication for a total of 8 min. Insoluble cellular debris was removed by centrifugation at 10,000 g for 1 h and the supernatant was loaded onto a Talon affinity column (10 × 1.25 cm) that had been preequilibrated with 10 column volumes of 50 mM KPi, 100 mM NaCl, and 10 mM imidazole, pH 7.4. The column was washed with 150 mL of the same buffer prior to bound proteins being eluted with a 400 mL linear gradient from 10 to 300 mM imidazole in 50 mM KPi, 100 mM NaCl, pH 7.4. The eluant was collected as 5 mL fractions. Fractions exhibiting significant absorption at 280 nm were pooled and FAD (100-150 μM) was added and the sample incubated for  $\sim 10$  min. Pure protein samples were buffer exchanged at 25°C into 50 mM KPi, pH 7.4 and concentrated using Amicon Ultra-15, 10 kDa nominal molecular weight cutoff centrifugal filters. The concentrated samples were quantified by absorption and stored at  $-80^{\circ}$ C as  $\leq 1$  mL aliquots of 200–300  $\mu$ M SmTGR. Prior to experiments individual SmTGR stocks were thawed on ice. To remove, what is assumed to be, precipitated SmTGR apoenzyme the sample was heated to 55 °C in a heating block for 5 min and centrifuged at 10,000 g for 15 min.

Anaerobic methods: Anaerobic kinetic analysis of SmTGR variants was undertaken using a HiTech stopped-flow spectrophotometer (TgK Scientific). Proteinaceous solutions were made anaerobic in glass tonometers. Dissolved dioxygen was exchanged for argon gas by cycling between vacuum and low pressure high purity argon 35 times whilst attached to a Schlenk line [17]. Non-proteinaceous solutions that included small molecule substrates and products were made anaerobic in buffer by sparging for 5 min with argon and mounting onto the stopped-flow spectrophotometer. At least 3 h prior to experiments, the instrument was scrubbed of residual oxygen by the introduction of 1 mM glucose with 1 U/mL glucose oxidase from a glass tonometer. Directly prior to experiments this glucose/glucose oxidase solution was displaced by anaerobic buffer prepared by sparging with argon as described. As previously reported, the addition of glucose and glucose oxidase destabilizes SmTGR and as such enzymatic dioxygen scrubbing was not employed during experiments.

Anaerobic steady-state analysis of SmTGR variants: SmTGR variants ( $\sim\!1-2~\mu\text{M})$  were prepared in a tonometer as described above and mixed with anaerobic solutions containing 100  $\mu\text{M}$  NADPH and a defined concentration of oxidant substrate. For combinations of GSSG and NADPH the solution was prepared by sparging with argon gas as described above. For each, the steady-state rate was defined between 20 and 60 s. The measured rates were divided by the SmTGR variant concentration and plotted against oxidant concentration and then fit to the Michaelis-Menten equation (Equation (1)), using KaleidaGraph software. In this equation Av. TN is the average turnover number calculated by dividing the measured rate in units of concentration per unit time by the enzyme concentration. Av. TN is used in place of [e]/v and TN in place of kcat as an acknowledgement that the fraction of active enzyme

was not determined for these data.

$$Av. TN = \frac{TN [S]}{K_m + [S]}$$
 Equation 1

Single turnover analysis of SmTGR variants with GSSG as the oxidant substrate: The influence of GSSG on the kinetics of singleturnover reactions was analyzed using anaerobic transient-state methods. Substrate solutions, containing limiting NADPH (U597C, 28  $\mu$ M; U597C + C31S, 23  $\mu$ M) with respect to the enzyme concentration and a range of concentrations of GSSG (U597C, 0, 25, 50, 100, 1000,  $2500 \ \mu M; \ U597C + C31S, \ 0, \ 25, \ 50, \ 1000, \ 2000 \ \mu M),$  were mixed with  $28~\mu M$  SmTGR U597C or  $23~\mu M$  SmTGR U597C + C31S and the reaction observed using stopped-flow spectrophotometry. The reaction was monitored at 460 nm for two timeframes, 0.0012-0.2 and 0.0012-2000 s. The two data sets for each concentration were spliced together at 0.2 s to provide adequate temporal resolution. This wavelength reports the net extent of oxidation of the FAD additive with the absorption of the FAD-thiolate charge transfer [15]. The data obtained were fit analytically to a linear combination of exponentials according to Equation (2) using Kaleidagraph Software (Synergy Software), where X is the wavelength of observation,  $A_n$  is the amplitude associated with phase n,  $k_{obsn}$ is the observed rate constant for phase n, t is time in s and C is the absorbance end point. The data were also fit to a kinetic model that incorporated binding competition between the C-terminal disulfide and GSSG using numerical integration in KinTek Explorer software (KinTek

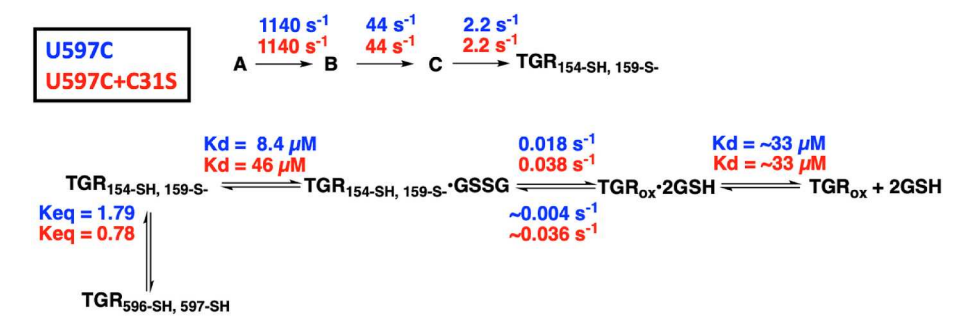
$$A_{Xnm} = \left(\sum_{n=1}^{X} \Delta A_n \left(e^{-k_{obsn}t}\right)\right) + C$$
 Equation 2

Transient state SmTGR U597S glutathione reductase activity. In the absence of oxidants, the U597S variant of TGR prevents electrons from NADPH from moving beyond the Cys154, Cys159 thiol pair. For this reason, this variant stabilizes the FAD-thiolate charge transfer formed when Cys159 is deprotonated by an adjacent histidine (His571) [15] and provides an observational signal for GSSG-induced decay of this absorption where GSSG acts as the oxidant that reforms the 154-159 disulfide, eliminating the FAD-thiolate charge transfer absorption (Fig. 1). This observation was achieved using double-mixing stopped-flow spectrophotometry under anaerobic conditions. SmTGR U597S (15  $\mu$ M) was initially mixed with NADPH (14  $\mu$ M) and the solution was aged for sufficient time to accumulate the FAD-thiolate charge transfer absorption (0.1 s) [15]. This was then mixed with 0-1280 μM GSSG and the oxidation of the enzyme/loss of FAD-thiolate CT signal was monitored at 540 nm. The traces were the average of at least two observations and were fit analytically to two exponentials according to Equation (2). The  $k_{2obs}$  values determined for the 160–1280  $\mu$ M GSSG concentrations were plotted against the oxidant concentration and the data was fit to Equation (3) to define the limiting rate of oxidation of the 154-159 dithiol and obtain an estimate for the SmTGR<sub>FAD-thiolate</sub>•GSSG complex binding constant (K<sub>GSSG</sub>). The data at GSSG concentrations above 40 μM were also fit globally by numerical integration to the competitive model shown in Scheme 1, assuming pre-formation of the FAD-thiolate absorption (TGR $_{154\text{-SH.}}$   $_{159\text{-S-}}$ ). Data below 40  $\mu\text{M}$  were either incomplete or include evidence of slow disproportionation and were not fit.

$$k_{2obs} = \frac{k_2[\text{GSSG}]}{K_{GSSG} + [\text{GSSG}]}$$
 Equation 3

### 3. Results

Anaerobic steady-state analysis of SmTGR variants: TGR enzymes are unique among the FDR family of enzymes as they catalytically reduce two oxidant substrates. Anaerobic transient-state and steady-state analyses have indicated that reduction of GSSG by SmTGR U597C occurs considerably more slowly than the reduction of Trx [16].



Scheme 1. Kinetic Model for SmTGR Turnover with Glutathione. This model accounts for all observed phases in the single turnover reaction of SmTGR with glutathione as the oxidant substrate. Initial steps involved in the reductive half reaction are included as first order irrevesible reactions to return observed rate constants for parts of the reaction that are unaltered by the addition of GSSG. The steps involved in reoxidation of the enzyme have been annotated with the relevant rate constants or equilibrium constants in blue (U597C) or red (U597C + C31S). Where equilibrium constants are reported, the fit was only sufficient to establish a lower limit of the rate constant, and no information about the intrinsic rate constant was accessible from these datasets.

Furthermore, the limiting rate of turnover of SmTGR U597C with GSSG is approximately equal to the limiting rate of FAD-thiolate oxidation observed with the U597S variant (see below). These two observations implicate disulfide exchange to form 2GSH as the slowest process in the catalytic cycle of SmTGR U597C. To investigate the site of GSSG reduction, steady state analyses were undertaken using the U597C, U597S, U597C + C31S, and I592STOP variants with GSSG as the oxidant. In this series, the U597C variant represents the functional enzyme with all disulfide exchange reactions intact. The U597S variant prevents electrons moving beyond the Cys154, Cys159 dithiol pair [15], and, based on prior claims for SmTGR, should prevent reduction of either oxidant substrate. The inability of the U597S variant to catalytically reduce Trx has been demonstrated [15]. And accordingly, the U597C + C31S variant would be predicted to prevent reduction of GSSG at the N-terminal Grx-fold domain (Fig. 1) while retaining the capacity to reduce Trx.

Anaerobic steady-state data for the SmTGR U597C and U597S variants indicate, within error, equivalent turnover numbers (0.025  $\pm$ 0.002, 0.026  $\pm$  0.001  $s^{-1})$  and  $K_M$  (170  $\pm$  40  $\mu M,$  200  $\pm$  20  $\mu M) values$ for both enzymes (Fig. 2). This is sound evidence that reduction of the Cys596-Sec597 sulfide-selenide pair is not required for SmTGR to reduce GSSG and that the disulfide exchange relay in SmTGR does not, in normal turnover, extend to catalytic reduction of GSSG at the Cys28, Cys31 dithiol pair. This is consistent with observations made for SmTGR with a two-residue C-terminal truncation, eliminating Sec597 residue, that was reported to retain the capacity to reduce GSSG, albeit observed under aerobic conditions [8]. Steady-state data obtained for the SmTGR U597C + C31S variant indicate a turnover number that is approximately 3-fold higher (0.08  $\pm$  0.01  $\mbox{s}^{-1}\mbox{)}$  and a  $\mbox{K}_{M}$  that is approximately 3-fold lower (60  $\pm$  10  $\mu M)$  than the U597C variant indicating a significant increase in catalytic efficiency and reinforcing that the Cys28, Cys31 dithiol pair is not required to reduce GSSG.

Single turnover kinetics of the SmTGR variants with GSSG as the oxidant substrate: The reduction of glutathione by SmTGR variants (U597C or U597C + C31S) was observed in the transient-state with limiting NADPH and varied concentrations of GSSG. The introduction of GSSG increases the rate of the final phase observed at 460 nm, titrating to a limit at the highest concentrations of GSSG. These data report the extent of oxidation of the flavin and given that fractional reduction of the flavin persists throughout the observation, indicate that all steps in the process are reversible [16]. Each data set was fit to a linear combination of exponentials and to a kinetic model that accounts for GSSG competing with the C-terminus for access to the Cys154, Cys159 dithiol pair using numerical integration fitting (Scheme 1). The initial stages of the reaction include NADPH binding, reduction of the enzyme, and NADP<sup>+</sup> release but these steps are included as part of the model only as individual irreversible steps (A $\rightarrow$  B $\rightarrow$ C $\rightarrow$ TGR<sub>154-SH, 159-S-</sub>) such that the fit returns observed rate constants for each of these initial phases. The

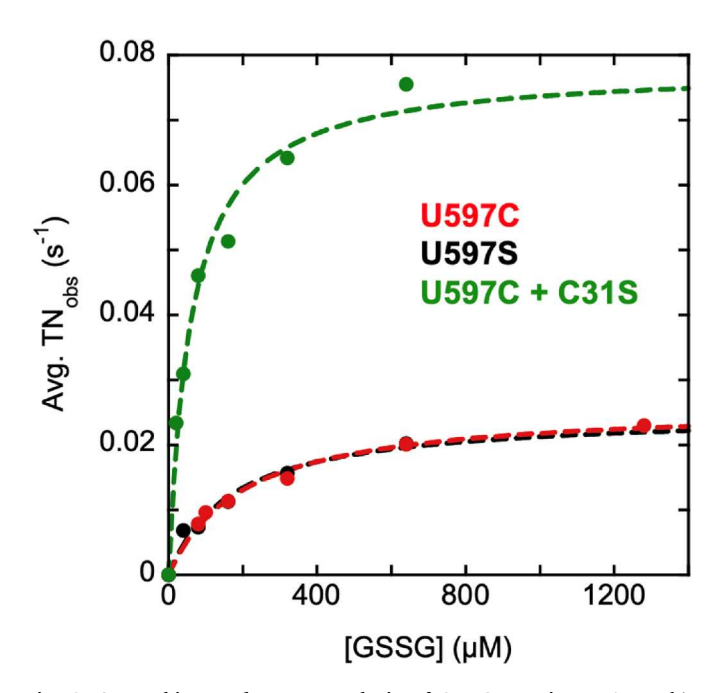


Fig. 2. Anaerobic steady state analysis of SmTGR variants. Anaerobic steady state turnover of SmTGR U597C (Red), U597S (Black), and U597C + C31S (Green) with GSSG as the oxidant substrate. SmTGR (U597C 1  $\mu M$ , U5975  $1.8~\mu M$ , U597C + C31S  $2.1~\mu M$ ) was mixed with NADPH (100  $\mu M$ ) and varied GSSG (0–1280  $\mu M$ ) and the oxidation of NADPH was measured at 340 nm. The data from 20 to 60 s was used to define the average rate of turnover at each oxidant concentration, which was then plotted against GSSG concentration and fit to the Michaelis-Menten equation (Equation 1).

basis for this is that these phases of the reaction are unchanging with GSSG concentration and so cannot be used to accurately determine the ratio of rates that comprise equilibria (Fig. 3). Based on prior reported observations these steps describe flavin reduction (1140 s $^{-1}$ ), FAD thiolate charge transfer accumulation (44 s $^{-1}$ ) and an initial step in flavin reoxidation for which the chemistry is, as yet, undefined (2.2 s $^{-1}$ ). A key feature of the model is that in the Cys154, Cys159 dithiol state (TGR<sub>154-SH, 159-S-</sub>), the electrons can be transferred either to GSSG or to the Cys596-Cys597 disulfide and that the occupancy and reduction of the C-terminus precludes the possibility of GSSG binding and reduction such that GSSG and the C-terminal disulfide compete as oxidants of the Cys154, Cys159 dithiol state. The fits obtained do not conform perfectly to the data, however they reflect trends in the rates and amplitudes of the data faithfully. Deviation from the model presumably arises from promiscuity of the disulfide exchange reactions that is unaccounted for

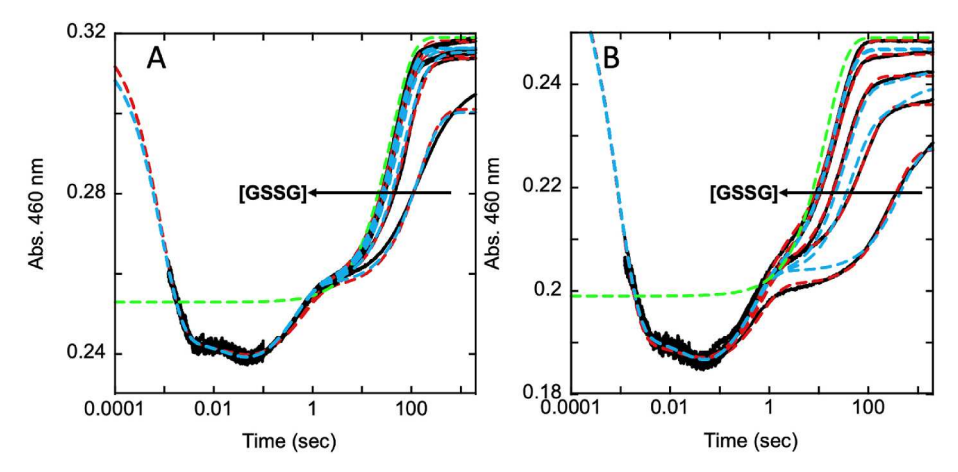


Fig. 3. Single turnover kinetics of SmTGR with GSSG as the oxidant substrate. SmTGR A) U597C ( $28 \mu M$ ) or B) U597C + C31S ( $23 \mu M$ ) was mixed with NADPH (U597C,  $26.4 \mu M$ ; U597C + C31S,  $24 \mu M$ ) and oxidized glutathione ( $0.25, 50, 100, 1000, 2500 \mu M$ ) under anaerobic conditions at  $20 \, ^{\circ}$ C. The reaction was observed at  $460 \, \text{nm}$  for two time frames ( $0.0012-0.2 \, \text{and} \, 0.0012-2000 \, \text{s}$ ) and the  $2000 \, \text{s}$  traces shown were spliced together at  $0.2 \, \text{s}$  to provide adequate time resolution for all phases. Arrows indicate increasing GSSG concentration. The blue dashed lines are simulated absorbance values at  $460 \, \text{nm}$  from 0 to  $2000 \, \text{s}$  derived from numerical integration fitting of the data to a branched multi-step model (Scheme 1). The red dashed lines are analytical fits to a linear combination of four exponentials, according to Equation (2). The green dashed lines indicates the limiting rate of turnover as measured in Fig. 2 ( $0.025 \, \text{s}^1$  for U597C ( $4.6 \, \text{m}$ ) and  $0.08 \, \text{s}^1$  for U597C + C31S ( $4.6 \, \text{m}$ ).

in the model, such as the previously described inter-protein disproportionation [16]. Given that the rate of the final phase is dependent on the concentration of GSSG, it is concluded that conversion of GSSG to 2GSH effectively defines the observed turnover number for the glutathione reductase activity of both SmTGR variants and that the additive values for forward and reverse steps in GSSG reduction derived from the fit for the U597C and U597C + C31S variants are 0.022  $\rm s^{-1}$  and 0.082  $\rm s^{-1}$  respectively and agree well with the measured turnover numbers for these variants (0.024  $\rm s^{-1}$  and 0.071  $\rm s^{-1}$ , cf. Figs. 2 and 3). The fit of these data to the model shown in Scheme 1, while descriptive, does offer support for the proposal that the C-terminus and GSSG compete for access to the Cys154, Cys159 dithiol state of the enzyme. The dissociation constants for GSSG to the reduced enzyme determined from the fit are  $\sim$ 8.4  $\mu$ M for U597C and  $\sim$ 46  $\mu$ M for U597C + C31S.

A matter that must be addressed to account for our current observations is that we previously reported that the addition of GSSG does not alter transient state single turnover observations [16]. However, as can be seen in Fig. 3, it is evident that GSSG does alter the kinetics of single turnover reactions causing a concentration dependent increase to a limit in the rate of the final phase observed. In the development of this project, a recurring issue has been a fraction of quasi-stable apo- and/or incorrectly folded SmTGR in the purified enzyme samples. It has been shown that reduced TGR has a propensity for disproportionation, presumably made possible by the dynamic behavior of the Cys596, Sec597 sulfhydryl, selenol [16]. The purification protocol reported here has been refined to eliminate this copurifying apo-enzyme contaminant. As such, it is conceivable that our initial attempts to characterizing the interaction of GSSG with SmTGR U597C in the transient-state were hindered by a significant fraction of inactive disulfide laden protein that acted as the dominant oxidant, outcompeting GSSG, resulting in no modulation of the observed flavin reoxidation kinetics by GSSG. This is supported by the fact that in our initial report, the observed rate constant of the final phase in transient state in the absence of GSSG fell between 0.016 and 0.05 s<sup>-1</sup>, substantially more rapid than the rates measured in this study of  $\sim 0.008 \text{ s}^{-1}$  [16].

Direct transient state observation of SmTGR U597S FAD-thiolate state oxidation by glutathione: The U597S variant of SmTGR severs the internal disulfide exchange relay. The Sec597, Cys596 selenide, sulfide is the redox active component of a proposed dynamic C-terminus that is thought to bridge between the static positioning of the Cys154, Cys159 disulfide adjacent to the flavin, the disulfide of bound Trx, and the Cys31, Cys28 disulfide near the proposed catalytic GSSG binding site

(Fig. 1). Mutating the U597 residue to serine renders the C-terminus unreactive for disulfide exchange reactions and halts the passage of electrons from NADPH at the Cys154, Cys159 dithiol state. Deprotonation of Cys159 by His571 (of the adjacent subunit) forms a thiolate that exhibits prominent charge transfer transitions with the adjacent oxidized FAD isoalloxazine [15,16]. This stabilized absorption signal in the U597S variant was used to assess whether GSSG interacts with and oxidizes the Cys154, Cys159 dithiol. SmTGR U597S was mixed with NADPH to form the FAD-thiolate charge transfer signal and then mixed with varied concentrations of GSSG. The data obtained shows GSSG dependent decay of the FAD-thiolate absorption (Fig. 4). The traces fit individually to two exponential shapes but as a set are complex and not described well by numerical integration fitting to a simple binding, oxidoreduction and release model. However, the second phase includes the majority of the amplitude change and the dependence of this phase clearly indicates saturation to a limit of 0.02 s<sup>-1</sup>, ostensibly the same as the limiting rate observed in steady state and transient state single turnover for the U597S and U597C variants with GSSG as the oxidant substrate (Figs. 2 and 3). In addition, the apparent dissociation constant (120 µM, based on fits only to the data obtained for pseudo-first order reactant ratios) agrees well with the K<sub>M</sub> values determined in the steady state for the U597S and U597C variants. However, this  $K_d$  value is ~15-fold higher than the value for this complex determined in transient state single turnover with the U597C variant (Fig. 3). When the data at higher concentrations of GSSG are fit using numerical integration to the model in Scheme 1, which accounts for competitive binding of the C-terminus, a  $K_d$  of  $\sim 10 \, \mu M$  is obtained, consistent with the value from the U597C transient state single turnover. The traces corresponding to lower concentrations of GSSG deviate significantly from this model, likely arising from disproportionation that is unaccounted for in the model.

Kinetic analysis of the I592STOP variant: The proposed competition between GSSG and the C-terminus for access to the thiol-thiolate state of Cys154-Cys159 was investigated by truncation. Seven residues were excluded from translation by mutagenesis to include a stop codon in place of Ile592. This variant form of SmTGR (I592STOP) was examined in steady state by mixing 2  $\mu M$  enzyme with varied GSSG concentrations in the presence of 100  $\mu M$  NADPH under anaerobic conditions. These data indicated the enzyme was unable to turnover and catalytically reduce GSSG (data not shown). To ascertain where in the catalytic cycle the variant enzyme fails, transient state single turnover experiments were conducted in which 27  $\mu M$  SmTGR I592STOP variant was

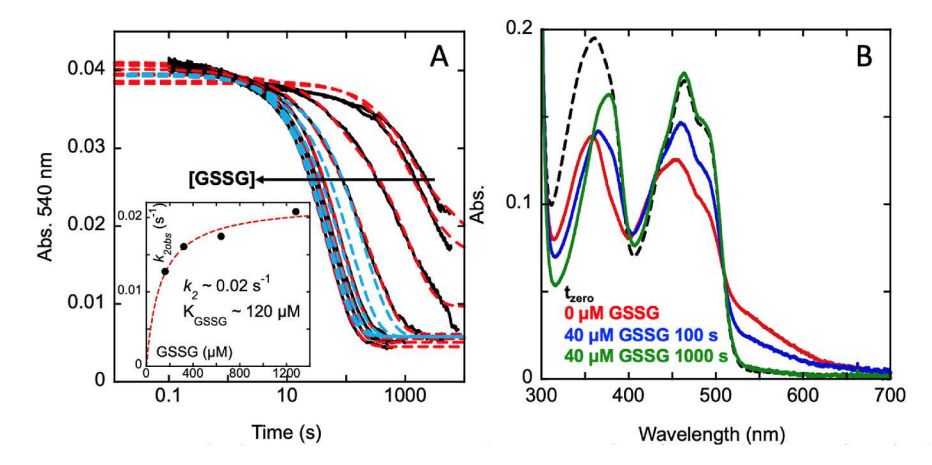


Fig. 4. TGR U5975 glutathione reductase activity. For A. and B., TGR U597C (15  $\mu$ M) was mixed with NADPH (14  $\mu$ M) and the solution was aged for 0.1 s to accumulate the FAD-thiolate charge transfer absorption. This was then mixed with 0, 10, 20, 40, 160, 320, 640, 1280  $\mu$ M GSSG and the reoxidation of the enzyme/loss of FAD-thiolate CT signal was monitored. A. The reoxidation of the enzyme was monitored at 540 nm and these traces were fit to two exponentials according to Equation (2) (red dashed lines). The k2obs values obtained for the pseudo-first order GSSG concentrations (160–1280  $\mu$ M) were plotted against the oxidant concentration and the data were fit to Equation (3). The data at high concentrations of GSSG were also fit using numerical integration to the model in Scheme 1 (blue dashed lines). Arrow indicates increasing GSSG concentration. B. Depicts the spectra collected as the reaction precedes, transitioning from the tzero spectrum (black dashed line), the first spectrum collected after TGR and NADPH were mixed (red spectrum), and the spectra collected 100 s (blue) and 1000 s (green) after the introduction of 40  $\mu$ M GSSG.

mixed with 27  $\mu M$  NADPH in the absence and presence of 50  $\mu M$  GSSG, 50  $\mu M$  GSSG with 50  $\mu M$  Cys, or 50  $\mu M$  Trx. Combining the enzyme with NADPH alone resulted in the reduction of the flavin and accumulation of FAD-thiolate charge transfer state. This indicated that the enzyme was competent to conduct the initial stages of catalysis but was unable to participate in disulfide exchange reactions.

The inability of the I592STOP variant to react with GSSG is unexpected and implicates involvement of the C-terminus in the reaction. The addition of GSSG does not alter any observed rates, the final net oxidation state of the enzyme nor does it perturb the FAD-thiolate absorption spectrum (Fig. 5), indicating that the I592STOP mutation renders SmTGR completely inert towards GSSG. That the U597S variant retains the GR activity observed in the U597C variant but the I592STOP variant is completely inactive dictates that Cys596 is necessary for GSSG reduction. Cysteine was added in modest concertation as a potential resolving thiol to rescue the GR activity that was lost upon removal of Cys596, however no activity was regained with the introduction of cysteine. As expected, the I592STOP variant showed no evidence of TrxR activity (Fig. 5a).

#### 4. Discussion

Electron transfer within SmTGR has been proposed to follow a branched disulfide exchange relay. In this model, electrons from NADPH enter the enzyme by hydride transfer to the FAD and are transferred to the proximal Cys154-Cys159 disulfide. The electrons are then transferred to the mobile, C-terminal Cys596-Sec597 sulfide-selenide and oxidant substrates become reduced by disulfide exchange with the thiol, selenol state of the C-terminus (Cys596, Sec597) (Fig. 1). The C-terminus carrying the thiol, selenol is proposed to be dynamic and stochastically distributive, either reducing the disulfide of thioredoxin bound  $\sim\!20~\text{Å}$  from the flavin or extending to bridge the  $\sim\!45~\text{Å}$  gap to the Cys28-Cys31 disulfide of the Grx domain, which in turn reduces oxidized glutathione. In this study we perform anaerobic kinetic analyses of several variant SmTGRs, each targeted to assess the involvement of the Cys28, Cys31 pair of the appended Grx domain in the catalytic reduction of glutathione.

It is widely reported that TGR catalyzes the reduction of GSSG, however the mechanism of this reduction, and the closely related Grx activity, has been a matter of persisting conjecture for which certainty

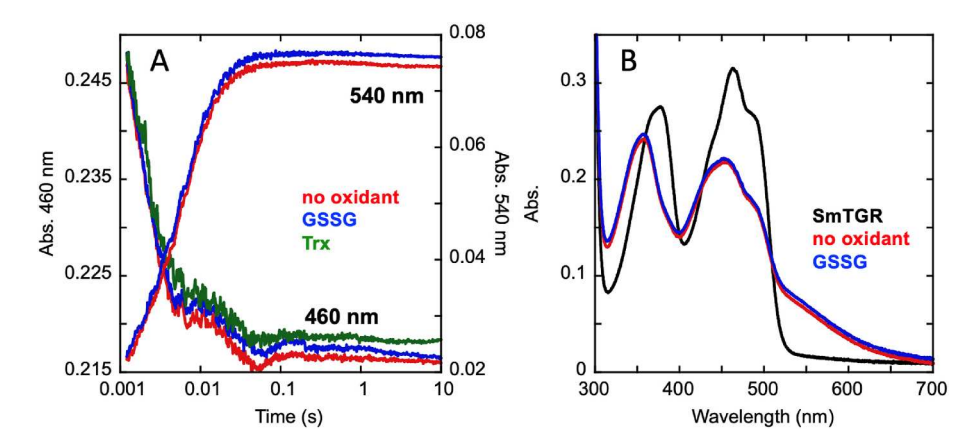


Fig. 5. Transient state analysis of the 1592STOP SmTGR variant. SmTGR 1592STOP variant (27  $\mu$ M) (black) was mixed with NADPH (27  $\mu$ M) in the absence (red) and presence of 50  $\mu$ M GSSG (blue), or 50  $\mu$ M Trx (green). A. Traces observed at 460 and 540 nm. Individual lines were separated by 0.001 AU for clarity. B. Endpoint spectra of specific reactions shown in A. relative to oxidized SmTGR 1592STOP. The spectrum that included GSSG was separated from the no oxidant spectrum by adding 0.003 AU to make it discernible from the no oxidant spectrum.

has been undermined by routine use of aerobic conditions for observations. Alger and Williams were the first to report the glutathione reductase (GR) and Grx activities of SmTGR [18]. Subsequently, Angelucci et al. showed crystallographically that the N-terminal domain of SmTGR closely resembles the fold of Grxs. Upon truncating the enzyme by removing the C-terminal Sec597-Gly598 motif, the enzyme was reported to retain Grx activity, establishing that the N-terminal domain is indeed a functional, independent Grx [19]. They also reported that the truncated SmTGR retained fractional GR activity, contrary to observations made with a similarly truncated mouse or human TGRs [19–21]. Based on these observations and the structural similarity of TGR with GRs, they posited a dual mode of GSSG reduction in which the predominant site of GR activity with SmTGR is the N-terminal Grx domain with residual GSSG reduction occurring directly at the Cys154, Cys159 pair [19].

Angelucci et al. later refined their assignment observing that U597C SmTGR does not have GR activity and concluded that most GR activity occurs in the N-terminal Grx domain. They attributed the diminishment in activity between the truncated and U597C variants to an increase in competition for binding between the C-terminus and GSSG, in the Sec597Cys variant that isn't possible in the truncated form [20]. The authors reasoned that the C-terminal Sec-Gly motif is structurally comparable to the Cys-Gly moiety of glutathione and would compete for binding at any site that glutathione binds. Further evidence for their assignment was provided by a structure of the SmTGR U597C•GSH complex, in which GSH was observed bound adjacent to the Cys28, Cys31 pair within the Grx domain [20]. Huang et al. then corroborated this mechanistic assignment using mutagenesis and showed that mutation of Cys28 to alanine or serine results in 3-4% GR activity relative to the WT enzyme, with the residual activity being attributed to the Cys154, Cys159 pair [22]. They also observed that mutating Cys31 to serine resulted in a faster rate of GSSG reduction, which they ascribed to reduced substrate inhibition arising from glutathionylation of this residue. Based on these observations, it was concluded that the preponderance of GR activity in SmTGR occurs at the N-terminal Grx domain.

The consensus therefore is that for TGR the major fraction of GR activity occurs at the Grx domain [23]. The data supporting this claim, however, are ambiguous as all conclusions drawn from kinetic observations were made from measurements conducted aerobically. We have shown previously that reduced states of SmTGR U597C have significant oxidase activity and consume NADPH aerobically with or without oxidant substrates [15,16]. This off-pathway activity undermines the capacity to measure relative rates or know stoichiometry with certainty. Here, we have made stringent anaerobic kinetic measurements for a series of SmTGR variants to demonstrate that the specific GR activity of SmTGR U597C is confined to the Cys154, Cys159 pair.

Steady-state analysis of the U597C, U597S, and U597C + C31S variants demonstrated that the Cys28, Cys31 pair does not additively contribute to the catalytic reduction of glutathione. The U597C variant contains a full complement of redox active centers and has served as a proxy for the wild-type enzyme in numerous studies [4,13,18–21,23]. In contrast, the U597S variant effectively renders the Cys596-Sec597 disulfide redox inactive and in doing so isolates Cys28-Cys31 pair from the disulfide exchange relay (Fig. 1). That the U597C and U597S variants behave, within error, identically in the steady-state with GSSG as the oxidant substrate indicates that neither Cys596-Cys597 nor the Cys28-Cys31 disulfides is participating in the catalytic reduction of glutathione. This point is made very apparent in the U597C + C31S steady-state data, which, rather inexplicably, displays a 3-fold increase in turnover number and 3-fold decrease in  $K_{\mbox{\scriptsize M}}$  relative to the other two variants. A rationalization for this heightened catalytic efficiency in the U597C + C31S variant is that in the U597C and U597S variants the C-terminus associates near the Cys154-Cys159 disulfide and competes with GSSG for binding, but in the U597C + C31S variant the C-terminus can form a mixed-disulfide cross-link with Cys28 that is stabilized by the absence of the Cys31 nucleophile, effectively tethering the C-terminus away from the flavin and diminishing its capacity to compete with GSSG. This proposed decrease in competition would be expected to lower the  $K_M$  value for GSSG as was observed. However, this would seem to be at odds with the observation that the I592STOP variant has no capacity to reduce GSSG (Fig. 5). Irrespective of the uncertainty in the mechanistic basis for the increased rate of turnover, it is evident that the Cys28-Cys31 disulfide is not intimately responsible for the catalytic reduction of glutathione by SmTGR U597C.

Fitting single turnover datasets to a model that incorporates competition between GSSG and the C-terminal disulfide for access to the Cys154, Cys159 dithiol state returned qualitatively good fits that simulate the observed trends when GSSG is titrated in the presence of a fixed and limiting concentration of NADPH. Moreover, the limiting rates returned from the fit for saturating GSSG concentrations (as annotated in Scheme 1) recapitulate the turnover numbers measured in the steady state for the U597C and U597C + C31S variants (Fig. 2). The relative higher catalytic efficiency of the U597C + C31S variant compared to the U597C variant was unexpected and suggest that the C-terminal dithiol can extend to interact with the Cys28-Cys31 disulfide forming of a stable mixed disulfide with the C-terminal cysteines effectively eliminating the competition with GSSG for access to the Cys154, Cys159 dithiol. This proposal is borne out in the numerical integration fit that predicts less competition with the C-terminus defined by a smaller equilibrium constant to form the C-terminal dithiol complex at the FAD for the U597C  $\pm$ C31S variant (Scheme 1).

To further demonstrate that GSSG interacts with SmTGR at the Cys145, Cys159 pair rather than the proposed Cys28, Cys31 pair, the charge transfer signal generated upon reduction and deprotonation of the Cys154, Cys159 pair was used as a direct observational handle for GSSG reduction. The U597S variant was utilized as it limits the progression of electrons to the first disulfide/dithiol pair resulting in accumulation of a stable FAD-thiolate charge transfer absorption. The addition of GSSG induces a concentration dependent increase in the rate of decay of the thiolate-FAD charge transfer, accelerating the decay by several orders of magnitude to a limit of  $\sim 0.02 \text{ s}^{-1}(\text{Fig. 4A})$ ; consistent both with the turnover number measured in the steady-state and the slowest rate observed in the transient state during single turnover. This indicates that for the U597C variant the limiting rate of turnover observed for SmTGR with GSSG directly involves the Cys154, Cys159 pair. It can be seen in Fig. 4B that at the end of this process, in the presence of GSSG, the enzyme has returned ostensibly to its initial state, confirming that the observations made correspond to complete reoxidation of the flavin.

It is unclear why the U597S variant retains full GR activity relative to U597C while the I592STOP variant is inactive (Figs. 3 and 5). The implication is that Cys596 is necessary for GR catalysis, but no mechanism for its direct involvement is posited. As is seen in Fig. 6, the Cterminus of SmTGR occupies the predicted binding site of the liberated distal molecule of GSH. Assuming significant reversibility when both molecules of GSH are bound, supported by observation that the internuclear distance is shorter between the thiols of each GSH molecule than between the Cys154/Cys159 thiols, it is conceivable that the C-terminus is necessary to displace the proximal molecule of GSH. This would allow for the relatively less favorable resolution of the mixed disulfide by Cys159 and may account for the observation that truncation leads to inactivity but isosteric mutations retain activity.

It is evident from the data presented here that SmTGR U597C does catalyze the reduction of oxidized glutathione, but at a site distinct from the Grx domain disulfide. Glutathione reductase (GR) is the paradigm for disulfide reduction of glutathione using only an FAD cofactor and a single disulfide/dithiol pair, and the active site of HsGR is shown in Fig. 6. The architecture is very similar to that of SmTGR, with NADPH binding on the *re*-face of the isoalloxazine and a disulfide/dithiol pair (Cys58, Cys63 in HsGR) located on the *si*-face. In addition, overlay of GR with SmTGR indicates that the mobile C-terminus (shown in blue and periwinkle in Fig. 6) is, in the pose shown, positioned adjacent to this

Fig. 6. Relative positions of the C-terminus of SmTGR and the known binding site for GSSG in GR. Overlay of SmTGR C-terminus (PDB 7802) (blue and periwinkle secondary structure) and the HsGR NADP(H) GSH complex (green for protein, yellow for ligands) (PDB 1GRE). GSHMD refers to the mixed disulfide form. Residues superscripted with an asterisks are derived from the opposing subunit of the dimer. The black square encompasses the region shown at right.

site, presumably precluding the binding and reduction of GSSG at this site. In addition, with comparison of the GSSG binding site in GR and SmTGR the residues responsible for substrate binding in GR are, with the exception of Arg37 (which is a lysine in SmTGR), conserved in SmTGR (Fig. 7). This high level of similarity between the known GSSG reduction site in GR and the proposed site of GSSG reduction in SmTGR further extends our assignment of Cys154, Cys159 as the site of GSSG reduction. In sum, SmTGR retains the classic GR architecture with an appended C-terminus that facilitates thioredoxin reduction, ostensibly the same TrxRs. That the enzyme accomplishes both chemistries, distributing electrons from the cysteine pair most proximal to the FAD without direct catalytic involvement of the Cys28, Cys31 pair requires access for both the C-terminus and GSSG to the disulfide/dithiol most proximal to the

The limiting rates for GSSG reduction reported here for the U597C and U597S variants are modest. However, as the only anaerobic observations for TGR these data cannot be purposefully compared with any other published kinetic observations. For example, both the human TGR (HsTGR) and SmTGR U597C variant have been kinetically characterized in prior reports under aerobic conditions and the reported  $k_{cat}$  values for GSSG reduction are similar and  $\sim$ 5–10 fold higher than the values reported here [16,19,21]. While catalytic rate comparisons across phyla are unlikely to be conclusively relevant, mammalian TGRs also possess an N-terminal Grx domain with the positionally equivalent residue to C31 in SmTGR as a native serine [24] and it has been reported that the Grx domain is required for GSSG reduction activity. Interestingly, no GSSG activity was observed for the U642C variant of HsTGR (functionally and positionally equivalent to the SmTGR U597C variant) suggesting that the selenocysteine has an integral role in GSSG activity in this form of the enzyme [21]. These apparently disparate observations typify much of the ambiguity within the TGR and, more broadly, the FDR literature. After five decades of enzymological observations many contradictory or inconsistent claims pervade the record of FDR enzymes. As we have argued above, the frequent deficiency in approach has been lack of experiments that demonstrate the propensity to reduce dioxygen prior to conducting kinetic experiments with native substrate oxidants under aerobic conditions (that introduces ~250 µM dissolved molecular oxygen) [10]. For this reason, the slow rate of GSSG reduction observed here for the U597C and U597S variants (0.02 s<sup>-1</sup>) cannot be contested or validated by any other reported observation made with a TGR or TrxR enzyme or one carrying the equivalent mutations at position 597. As concession, the interplay of participating residues for transmittance of electrons within TGR enzymes is not explicitly known, so our observations may not speak to a unique catalytic role of the Sec597 residue in the reduction of GSSG by SmTGR. In our hands the rate of Trx reduction by SmTGR U597C is ~5-fold more rapid than GSSG reduction activity [16]. It is therefore conceivable that the GSSG reduction activity we have observed is a vestige of the structural lineage of the TGR enzymes and not representative of a native SmTGR GSSG reduction activity that is reliant on the participation of the Sec597 residue. Despite the lack of validation, the data presented are an internally consistent set of observations made in the absence of dioxygen reduction and so are currently the only definitive observations made for GSSG activity in a TGR enzyme. We would posit that the lack of additive contribution to the rate comparing the U597C and the U597S variants is sound evidence that the Grx domain is not the site of GSSG reduction.

# **Funding sources**

This work was supported by the National Science Foundation Grant

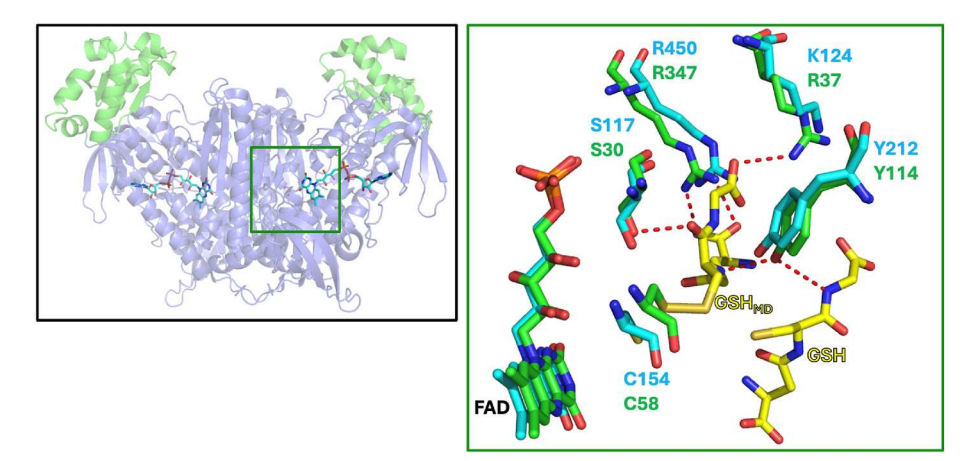


Fig. 7. Conservation of the glutathione binding pocket in SmTGR. At left is the structure of SmTGR (PDB  $2 \times 8C$ ) and the green square encompasses the region shown at right. Overlaid and aligned are the structures of glutathione bound Homo sapien Glutathione Reductase (PDB 1GRE) and SmTGR (PDB 2X8C). The residues responsible for glutathione binding in HsGR are shown in green, with apparent hydrogen bonds to the GSH products depicted as dashed red lines. The blue residues are the homologous residues in SmTGR. GSHMD refers to the mixed disulfide form of GSH.

CLP- 2203593 to G.R.M.

## CRediT authorship contribution statement

**Tyler B. Alt:** Writing – review & editing, Writing – original draft, Validation, Methodology, Formal analysis, Data curation, Conceptualization. **Madison M. Smith:** Writing – original draft, Visualization, Validation, Investigation, Formal analysis, Data curation, Conceptualization. **Graham R. Moran:** Writing – review & editing, Writing – original draft, Visualization, Supervision, Software, Resources, Project administration, Methodology, Funding acquisition, Formal analysis, Data curation, Conceptualization.

#### Data availability

Data will be made available on request.

#### References

- [1] D. Montero, C. Tachibana, J. Rahr Winther, C. Appenzeller-Herzog, Intracellular glutathione pools are heterogeneously concentrated, Redox Biol. 1 (1) (2013) 508–513
- [2] O. Goldbeck, A.W. Eck, G.M. Seibold, Real time monitoring of NADPH concentrations in corynebacterium glutamicum and Escherichia coli via the genetically encoded sensor mBFP, Front, Microbiol. 9 (2018) 2564.
- [3] H.M. Alger, D.L. Williams, The disulfide redox system of Schistosoma mansoni and the importance of a multifunctional enzyme, thioredoxin glutathione reductase, Mol. Biochem. Parasitol. 121 (1) (2002) 129–139.
- [4] A.N. Kuntz, E. Davioud-Charvet, A.A. Sayed, L.L. Califf, J. Dessolin, E.S. Arner, D. L. Williams, Thioredoxin glutathione reductase from Schistosoma mansoni: an essential parasite enzyme and a key drug target, PLoS Med. 4 (6) (2007) e206.
- [5] E.F. Pai, G.E. Schulz, The catalytic mechanism of glutathione reductase as derived from x-ray diffraction analyses of reaction intermediates, J. Biol. Chem. 258 (3) (1983) 1752–1757.
- [6] G. Waksman, T.S. Krishna, C.H. Williams Jr., J. Kuriyan, Crystal structure of Escherichia coli thioredoxin reductase refined at 2 A resolution. Implications for a large conformational change during catalysis, J. Mol. Biol. 236 (3) (1994) 800–816.
- [7] L. Zhong, E.S. Arner, A. Holmgren, Structure and mechanism of mammalian thioredoxin reductase: the active site is a redox-active selenolthiol/selenenylsulfide formed from the conserved cysteine-selenocysteine sequence, Proc Natl Acad Sci U S A 97 (11) (2000) 5854–5859.
- [8] F. Angelucci, A.E. Miele, G. Boumis, D. Dimastrogiovanni, M. Brunori, A. Bellelli, Glutathione reductase and thioredoxin reductase at the crossroad: the structure of Schistosoma mansoni thioredoxin glutathione reductase, Proteins 72 (3) (2008) 936–945.
- [9] F. Angelucci, D. Dimastrogiovanni, G. Boumis, M. Brunori, A.E. Miele, F. Saccoccia, A. Bellelli, Mapping the catalytic cycle of Schistosoma mansoni thioredoxin glutathione reductase by X-ray crystallography, J. Biol. Chem. 285 (42) (2010) 32557–32567
- [10] M.M. Smith, G.R. Moran, Building on a theme: the redox hierarchy of pyridine nucleotide-disulfide oxidoreductases, Arch. Biochem. Biophys. 755 (2024) 109966.
- [11] P.A. Karplus, G.E. Schulz, Refined structure of glutathione reductase at 1.54 A resolution, Journal of molecular biology 195 (3) (1987) 701–729.

- [12] K. Fritz-Wolf, E. Jortzik, M. Stumpf, J. Preuss, R. Iozef, S. Rahlfs, K. Becker, Crystal structure of the Plasmodium falciparum thioredoxin reductase-thioredoxin complex, J. Mol. Biol. 425 (18) (2013) 3446–3460.
- [13] H.H. Huang, L. Day, C.L. Cass, D.P. Ballou, C.H. Williams Jr., D.L. Williams, Investigations of the catalytic mechanism of thioredoxin glutathione reductase from Schistosoma mansoni, Biochemistry 50 (26) (2011) 5870–5882.
- [14] F.T. Ogata, V. Branco, F.F. Vale, L. Coppo, Glutaredoxin: discovery, redox defense and much more, Redox Biol. 43 (2021) 101975.
- [15] M.M. Smith, G.R. Moran, Assigning function to active site residues of Schistosoma mansoni thioredoxin/glutathione reductase from analysis of transient state reductive half-reactions with variant forms of the enzyme, Front. Mol. Biosci. 10 (2023) 1258333.
- [16] M.M. Smith, T.B. Alt, D.L. Williams, G.R. Moran, Descriptive analysis of transient-state observations for thioredoxin/glutathione reductase (Sec597Cys) from schistosoma mansoni, Biochemistry 62 (9) (2023) 1497–1508.
- [17] G.R. Moran, Anaerobic methods for the transient-state study of flavoproteins: the use of specialized glassware to define the concentration of dioxygen, Methods Enzymol. 620 (2019) 27–49.
- [18] H.M. Alger, D.L. Williams, The disulfide redox system of and the importance of a multifunctional enzyme, thioredoxin glutathione reductase, Mol. Biochem. Parasitol. 121 (1) (2002) 129–139.
- [19] F. Angelucci, A.E. Miele, G. Boumis, D. Dimastrogiovanni, M. Brunori, A. Bellelli, Glutathione reductase and thioredoxin reductase at the crossroad: the structure of thioredoxin glutathione reductase, Proteins: Struct., Funct., Bioinf. 72 (3) (2008) 036–045
- [20] F. Angelucci, D. Dimastrogiovanni, G. Boumis, M. Brunori, A.E. Miele, F. Saccoccia, A. Bellelli, Mapping the catalytic cycle of schistosoma mansoni thioredoxin glutathione reductase by X-ray crystallography, J. Biol. Chem. 285 (42) (2010) 32557–32567.
- [21] C. Brandstaedter, K. Fritz-Wolf, S. Weder, M. Fischer, B. Hecker, S. Rahlfs, K. Becker, Kinetic characterization of wild-type and mutant human thioredoxin glutathione reductase defines its reaction and regulatory mechanisms, FEBS J. 285 (3) (2018) 542–558.
- [22] H.H. Huang, L. Day, C.L. Cass, D.P. Ballou, C.H. Williams, D.L. Williams, Investigations of the catalytic mechanism of thioredoxin glutathione reductase from, Biochemistry 50 (26) (2011) 5870–5882.
- [23] V.Z. Petukhova, S.Y. Aboagye, M. Ardini, R.P. Lullo, F. Fata, M.E. Byrne, F. Gabriele, L.M. Martin, L.N.M. Harding, V. Gone, B. Dangi, D.D. Lantvit, D. Nikolic, R. Ippoliti, G. Effantin, W.L. Ling, J.J. Johnson, G.R.J. Thatcher, F. Angelucci, D.L. Williams, P.A. Petukhov, Non-covalent inhibitors of thioredoxin glutathione reductase with schistosomicidal activity in vivo, Nat. Commun. 14 (1) (2023) 3737.
- [24] D.M. Muzny, S.E. Scherer, R. Kaul, J. Wang, J. Yu, R. Sudbrak, C.J. Buhay, R. Chen, A. Cree, Y. Ding, S. Dugan-Rocha, R. Gill, P. Gunaratne, R.A. Harris, A.C. Hawes, J. Hernandez, A.V. Hodgson, J. Hume, A. Jackson, Z.M. Khan, C. Kovar-Smith, L. R. Lewis, R.J. Lozado, M.L. Metzker, A. Milosavljevic, G.R. Miner, M.B. Morgan, L. V. Nazareth, G. Scott, E. Sodergren, X.Z. Song, D. Steffen, S. Wei, D.A. Wheeler, M. W. Wright, K.C. Worley, Y. Yuan, Z. Zhang, C.Q. Adams, M.A. Ansari-Lari, M. Ayele, M.J. Brown, G. Chen, Z. Chen, J. Clendenning, K.P. Clerc-Blankenburg, R. Chen, Z. Chen, C. Davis, O. Delgado, H.H. Dinh, W. Dong, H. Draper, S. Ernst, G. Fu, M.L. Gonzalez-Garay, D.K. Garcia, W. Gillett, J. Gu, B. Hao, E. Haugen, P. Havlak, X. He, S. Hennig, S. Hu, W. Huang, L.R. Jackson, L.S. Jacob, S.H. Kelly, M. Kube, R. Levy, Z. Li, B. Liu, J. Liu, W. Liu, J. Lu, M. Maheshwari, B.V. Nguyen, G.O. Okwuonu, A. Palmeiri, S. Pasternak, L.M. Perez, K.A. Phelps, F.J. Plopper, B. Qiang, C. Raymond, R. Rodriguez, C. Saenphimmachak, J. Santibanez, H. Shen, Y. Shen, S. Subramanian, P.E. Tabor, D. Verduzco, L. Waldron, J. Wang, J. Wang, Q. Wang, G.A. Williams, G.K. Wong, Z. Yao, J. Zhang, X. Zhang, G. Zhao, J. Zhou, Y. Zhou, D. Nelson, H. Lehrach, R. Reinhardt, S.L. Naylor, H. Yang, M. Olson, G. Weinstock, R.A. Gibbs, The DNA sequence, annotation and analysis of human chromosome 3, Nature 440 (7088) (2006) 1194-1198.